J. Comp. Path. 2013, Vol. ■, 1–9

Available online at www.sciencedirect.com

SciVerse ScienceDirect

ELSEVIER

www.elsevier.com/locate/jcpa

EXPERIMENTALLY INDUCED DISEASE

Immunohistochemical Characterization of Type II Pneumocyte Proliferation after Challenge with Type I Porcine Reproductive and Respiratory Syndrome Virus

G. Balka*, A. Ladinig†, M. Ritzmann†,‡, A. Saalmüller§, W. Gerner§, T. Käser§, C. Jakab*, M. Rusvai* and H. Weißenböck¶

** Department of Pathology and Forensic Veterinary Medicine, Faculty of Veterinary Science, Szent István University, Budapest, Hungary, † Clinic for Swine, Department for Farm Animals and Veterinary Public Health, University of Veterinary Medicine, Vienna, Austria, ‡ Clinic for Swine, Ludwig-Maximilians University, Oberschleissheim, Germany, § Institute of Immunology, Department of Pathobiology and ¶ Institute of Pathology and Forensic Veterinary Medicine, University of Veterinary Medicine, Vienna, Austria*

Summary

The aim of this study was to characterize histologically and immunohistochemically the lung lesions developing in growing pigs, 10 and 21 days after experimental challenge with a field strain of porcine reproductive and respiratory syndrome virus (PRRSV). Lung lesions were scored for (1) pneumocyte hypertrophy and hyperplasia, (2) septal mononuclear infiltration, (3) intra-alveolar necrotic debris, (4) intra-alveolar inflammatory cell accumulation and (5) perivascular inflammatory cell accumulation. Immunohistochemistry was performed using antibodies specific for cytokeratin, Ki67, thyroid transcription factor (TTF)-1, the myelomonocytic marker MAC387 and PRRSV. Anti-TTF-1 identified type II pneumocytes and there was marked proliferation of these cells compared with control lung ($P < 0.05$). Anti-cytokeratin labelled type I and II pneumocytes as well as bronchial epithelial cells; however, this labelling was not suitable for cell counting purposes. There was a correlation between lesion severity and the number of cells expressing Ki67 ($P < 0.05$).

Keywords: pig; PRRSV; TTF-1; type II pneumocyte

Introduction

Porcine reproductive and respiratory syndrome (PRRS) is a globally important disease of swine that is characterized by reproductive loss in breeding animals and respiratory signs in young animals. The disease was first described in North America, and after appearing in Europe, PRRS spread all over the world causing marked economic loss. Analysis of the causative porcine reproductive and respiratory syndrome virus (PRRSV) revealed limited genetic relationship between the North American and European strains, so two genotypes were defined: European (type I) and American (type II) (Nelsen *et al*., 1999). Recent sequence analysis of Lithuanian, Belarussian and Russian strains led to the definition of four distinct subtypes within the European genotype (Stadejek *et al*., 2008). In 2006, a new and highly pathogenic (HP) PRRS emerged in China and Vietnam and, more recently, in other Southeast Asian countries including Bhutan, Cambodia, Laos, Malaysia, Myanmar, the Philippines, Thailand, Singapore, South Korea and also in Russia (Zimmerman *et al*., 2012). HP PRRS is characterized by high fever (41–42°C), skin haemorrhages, high morbidity (50–100%) and mortality (20–100%) in pigs of all ages. All HP PRRSV strains belong to genotype II, and although the disease has not been reported in

Correspondence to: G. Balka (e-mail: balka.gyula@aotk.szie.hu).

0021-9975/$ - see front matter

http://dx.doi.org/10.1016/j.jcpa.2012.12.006

Please cite this article in press as: Balka G, et al., Immunohistochemical Characterization of Type II Pneumocyte Proliferation after Challenge with Type I Porcine Reproductive and..., Journal of Comparative Pathology (2013), http://dx.doi.org/10.1016/j.jcpa.2012.12.006

Europe, a type I subtype III strain (the 'Lena' strain) causes high fever, anorexia, depression and 40% mortality in experimental infection (Karniychuk *et al.*, 2010).

PRRSV shows strong affinity for the lung and especially for its primary target cell, the alveolar macrophage. Both apoptotic and necrotic changes are observed in these cells, markedly decreasing the immunological defence in the lung. Additionally, cytokines and chemokines released by virus-infected cells contribute to damage to the lung parenchyma (referred to as a 'bystander effect') (Kim *et al.*, 2002; Miller and Fox, 2004; Lee and Kleiboeker, 2007). Microscopically, the infection is reported to cause interstitial pneumonia characterized by hyperplastic and hypertrophic type II pneumocytes, septal infiltration by mononuclear cells and accumulation of necrotic alveolar exudate (Halbur *et al.*, 1996; Rossow, 1998; Gómez-Laguna *et al.*, 2010).

Type II pneumocytes are cuboidal cells, located typically at the insertion of the alveolar septa. In mammalian lungs, type II pneumocytes constitute 60% of all alveolar epithelial cells, but cover only about 5% of the alveolar surface (Crapo *et al.*, 1982). Their most important role is the synthesis, secretion and recycling of pulmonary surfactant, which reduces alveolar surface tension, preventing collapse during expiration. The other important function of the type II pneumocytes lies in their proliferative potential. After injury of type I pneumocytes, type II pneumocytes serve as progenitor cells to replace and eventually differentiate into damaged and desquamated type I pneumocytes. Their phagocytic ability removes apoptotic type II pneumocytes and immunoregulatory activity occurs via interactions with macrophages and lymphocytes (Fehrenbach, 2000). Clara cells are non-ciliated, non-mucus-secreting progenitor cells that can proliferate and replace ciliated and other non-ciliated cells in the terminal part of the bronchi (Caswell and Williams, 2007).

Thyroid transcription factor (TTF)-1 is a 38 kDa homeodomain-containing nuclear protein and a member of the Nkx2 transcription factor family. The protein was originally described as a regulator of the thyroid-specific transcription of thyroglobulin, thyroperoxidase and thyrotropin receptor. In the lung, TTF-1 regulates surfactant gene and Clara cell secretory protein gene transcription (Bohinski *et al.*, 1994; Ray *et al.*, 1996; Zhou *et al.*, 1996). As TTF-1 is expressed in the nuclei of type II pneumocytes and Clara cells in the lungs, it is widely used as a marker for the diagnosis of primary and metastatic lung cancer (Tan *et al.*, 2003).

The aims of the present study were (1) to determine whether humanized anti-TTF-1 antibodies cross-react with porcine type II pneumocytes, (2) to determine whether PRRSV infection leads to proliferation of type II pneumocytes, and (3) to characterize the nature of the inflammatory lesions induced in the lung by PRRSV infection.

Materials and Methods

Twenty-four 8-week-old piglets were obtained from a conventional farm in lower Austria that was known to be free of PRRSV. The piglets were vaccinated against *Mycoplasma hyopneumoniae* and porcine circovirus type 2 at 3 weeks of age. Blood samples were taken from the animals at the time of arrival at the experimental unit and tested for antibodies against PRRSV by enzyme-linked immunosorbent assay (ELISA) and by quantitative reverse transcriptase polymerase chain reaction (RT-PCR) to confirm PRRSV negativity. After one week of acclimatization in an L3 safety level housing unit, 12 pigs were inoculated intranasally with 2.2×10^5 $TCID_{50}$ of type 1, subtype 1 virulent German PRRSV field isolate. The open reading frame (ORF)-5 nucleotide sequence of this isolate is 90% identical to that of the Lelystad type I reference strain (GenBank accession number M96262), while the glycoprotein (GP)-5 amino acid sequence is 92% identical to that strain. Negative control pigs ($n = 12$) were inoculated with virus-free cell culture supernatant. Animals were killed at 10 ($n = 7$) and 21 ($n = 5$) days post infection (dpi). During the course of the study, clinical signs, rectal temperature and average daily weight gain were monitored.

At necropsy examination, gross lung lesions (e.g. tan mottled areas or areas of consolidation) were scored by visual examination based on the percentage of each lobe affected (Halbur *et al.*, 1995). The percentage of lung lobe with lesions was used to calculate the total weighted lung lesion score. The Wilcoxon−Mann−Whitney test was used to investigate differences between the infected and control groups. Separate analyses were performed for mottled areas and for areas of consolidation.

Lung lobes were fixed in 10% neutral buffered formalin for 24 h at room temperature. Tissue specimens were dehydrated through a series of ethanol and xylene baths and embedded in paraffin wax. Sections (3−4 μm) were stained with haematoxylin and eosin (HE). For immunohistochemistry (IHC) the left medial lobes were analyzed to exclude the possible effect of different lesion distribution (the cranial and middle lobes invariably displayed more severe lesions than the caudal lobes).

For IHC, sections (3−4 μm) were mounted on SuperFrostPlus® slides (Menzel-Gläser, Braunschweig,

Please cite this article in press as: Balka G, et al., Immunohistochemical Characterization of Type II Pneumocyte Proliferation after Challenge with Type I Porcine Reproductive and..., Journal of Comparative Pathology (2013), http://dx.doi.org/10.1016/j.jcpa.2012.12.006

Germany). The slides were dewaxed in xylene and graded ethanol. Endogenous peroxidase activity was blocked by incubation with 3% H_2O_2 in methanol. After antigen retrieval (10 min at 95°C with EZ AR3 antigen retrieval solution, BioGenex, Fairmont, California, USA) and protein blocking with Power Block™ reagent (BioGenex, 10 min at room temperature), sections were treated with primary antibodies specific for cytokeratins (AE1 mouse monoclonal and AE3 mouse monoclonal; BioGenex; ready-to-use solution, 30 min at 37°C), Ki67 (clone BGX-Ki67 mouse monoclonal; BioGenex; ready-to-use solution, 1 h at 37°C), TTF-1 (clone BGX-397A mouse monoclonal; BioGenex; 1 in 100 dilution, 30 min at 37°C), the myelomonocytic marker MAC 387 (clone LS-C87783, mouse monoclonal; LifeSpan BioSciences, Seattle, Washington, USA; 1 in 500 dilution, 30 min at 37°C) and PRRSV SDOW-17/SR-30 (mouse monoclonal; Rural Technologies Inc., Brookings, South Dakota, USA; 1 in 500 dilution, 30 min at 37°C).

Secondary detection was performed using the Super Sensitive™ One-Step Polymer-HRP Detection System (BioGenex). The chromogen substrate was 3, 3′-diaminobenzidine tetrahydrochloride included in the kit. Mayer's haematoxylin was used for counterstaining.

Lesion severity and lesion distribution was scored as 0, no lesion; 1, mild; 2, moderate or 3, severe. Changes evaluated included (1) pneumocyte hypertrophy and hyperplasia, (2) septal mononuclear infiltration, (3) intra-alveolar necrotic debris, (4) intra-alveolar inflammatory cell accumulation and (5) perivascular inflammatory cell accumulation. The lesions were scored for all seven lung lobes (so the maximum score was 42 for each lesion. The microscopical evaluation was performed in a blinded fashion.

For Ki67, TTF-1 and MAC387 IHC the labelled cells were counted in 50 non-overlapping and consecutively-selected high magnification fields of 0.20 mm^2. Cell counts were compared between infected and control lungs. Cell counts were also compared with the overall histological score of the lung lobe.

PASW 17 (SPSS Inc., Chicago, Illinois, USA) software was used for statistical analyses. The student's t-test was used for significance calculations and Pearson's product-moment test was used to determine correlation.

Results

All control animals remained clinically healthy during the study and had no gross lesions at necropsy examination. The PRRSV negative status of this group was confirmed by consecutive serological and PCR tests throughout the study. Following challenge, an increase in rectal temperature was observed in the infected pigs with at least two or more pigs having a body temperature >40.5°C from 1 to 9 dpi. Coughing was observed in >60% of these animals. Within the first 9 dpi, uninfected animals showed a significantly higher body weight gain (6.8 kg) than that of the infected animals (3.9 kg, $P < 0.001$).

Tan mottled areas were observed with various distributions in the lungs of infected animals. No lesions or minimal lesions were present in the lungs of control animals, with a significant difference between the groups (Table 1).

There were significant differences ($P \leq 0.02$) in the presence and severity of microscopical lesions between challenged animals and the negative controls (Table 2). The greatest differences were in the presence of necrotic alveolar debris and in the intra-alveolar accumulation of inflammatory cells (predominantly neutrophils), in which a marked decrease was revealed between the acute (10 dpi) and chronic healing stages (21 dpi) of the disease. Necrotic debris and intra-alveolar inflammatory cells were almost totally absent in the lungs of uninfected animals; however, relatively high scores were given to the control lungs for this parameter relative to the other categories of change. By comparing the severity of the lesions at 10 and 21 dpi it was noted that the presence of intra-alveolar necrotic debris and intra-alveolar inflammatory cells decreased significantly with time; however, for the other categories of change only a minimal decrease in severity was registered (Fig. 1).

The TTF-1 antibodies successfully identified porcine type II pneumocytes in healthy and diseased lung tissues with homogenous and intense nuclear labelling. Epithelial cells of the bronchioli were also positive with stronger, more intense labelling of the non-ciliated Clara cells. Weaker, scattered positivity was observed among the cells of the bronchi. TTF-1-positive pneumocytes in healthy lungs were located predominantly at the insertion of the alveoli. The number of TTF-1-positive cells was significantly

Table 1
Weighted score (%) of tan mottled areas and areas of consolidation observed at necropsy for both groups at 10 and 21 dpi and combined for both time points

Group	*Days post infection*	*Mottled areas*	P *value*	*Consolidation*	P *value*
Control	Total	0.0		0.0	
Infected	Total	24.4	<0.002	44.5	<0.002
Control	10	0.0		0.0	
Infected	10	40.6	0.00	77.4	0.00
Control	21	0		0	
Infected	21	5.1	0.048	5.1	0.0484

Please cite this article in press as: Balka G, et al., Immunohistochemical Characterization of Type II Pneumocyte Proliferation after Challenge with Type I Porcine Reproductive and..., Journal of Comparative Pathology (2013), http://dx.doi.org/10.1016/j.jcpa.2012.12.006

Table 2
Mean and standard deviation for the five evaluated parameters, the total histological score and the IHC results from control and infected animals at 10 and 21 dpi

Group	*dpi*	*Total score*	*Pneumocyte hypertrophy and hyperplasia*	*Septal infiltration with mononuclear cells*	*Necrotic debris*	*Intra-alveolar accumulation of inflammatory cells*	*Perivascular accumulation of inflammatory cells*	*Ki67 IHC*	*Mac387 IHC*	*TTF-1 IHC*
Control	10	44.8 ± 16.3	6.5 ± 5.1	21.8 ± 3.7	0.3 ± 0.8	5.0 ± 3.7	11.2 ± 5.8	109.8 ± 13.7	98.0 ± 7.8	128.4 ± 7.5
Control	21	23.3 ± 7.0	1.3 ± 1.6	12.3 ± 4.5	0.0 ± 0.0	2.2 ± 4.4	7.5 ± 3.8	80.9 ± 23.9	69.7 ± 40.4	108.3 ± 18.0
Infected	10	129.0 ± 18.0	24.5 ± 4.2	28.5 ± 4.2	25.3 ± 6.3	26.3 ± 3.6	24.3 ± 4.1	124.9 ± 41.5	99.1 ± 23.0	142.7 ± 19.7
Infected	21	86.7 ± 19.3	188 ± 58	24.8 ± 5.1	7.5 ± 6.2	13.0 ± 6.1	22.5 ± 3.6	140.7 ± 45.2	92.7 ± 21.9	158.5 ± 36.9

dpi, days post infection; IHC, immunohistochemistry.

higher ($P < 0.05$) in the acute phase of infection than in the negative control lungs. The proliferative hallmark of the lesion was supported by strong up-regulation of Ki67-positive cells; however, the increase in labelling was not significant (Fig. 2). Similarly, the number of MAC387-positive macrophages showed an increase without statistical significance.

Cytokeratin labelling clearly identified the pneumocytes with homogenous and intense cytoplasmic reactivity. Type I pneumocytes were flattened cells lining the alveolar spaces, while type II pneumocytes were rounded cells usually located at the insertion of the alveolar spaces in control lungs. In infected animals, as verified by TTF-1 labelling, these rounded cells were found in markedly higher number.

The analysis of PRRSV labelled slides revealed only a few positive cells in animals of the first group (at 10 dpi) and minimal or no staining was observed at 21 dpi.

Discussion

Naturally occurring PRRSV infections are usually complicated by secondary bacterial and/or other viral infections. In the majority of cases, virus-induced immunosuppression and the impairment of local defence mechanisms result in such secondary infections and present as catarrhal-purulent lesions, especially in the cranial and cranioventral lungs.

Under experimental conditions PRRSV infection is reported to cause interstitial pneumonia characterized by the presence of hyperplastic and hypertrophic type 2 pneumocytes, septal infiltration by mononuclear cells and accumulation of necrotic alveolar exudate (Halbur *et al*., 1996; Rossow, 1998; Gómez-Laguna *et al*., 2010).

In the present experimental study all seven lung lobes were sampled and scored for the severity and distribution of the following histopathological lesions: (1) pneumocyte hypertrophy and hyperplasia, (2) septal mononuclear infiltration, (3) intra-alveolar necrotic debris, (4) intra-alveolar inflammatory cell accumulation and (5) perivascular inflammatory cell accumulation. Statistical comparison of the scores derived from infected and control pigs showed a significant increase for all five parameters and for the overall severity scores. A significant decrease in intra-alveolar necrotic debris and intra-alveolar inflammatory cells was observed at 21 dpi in infected pigs; in contrast, only minimal change was present for the other three categories. These findings can be explained by the fact that formation of intra-alveolar necrotic debris and subsequent accumulation of intra-alveolar inflammatory cells (predominantly neutrophils) reflects the acute phase of the disease,

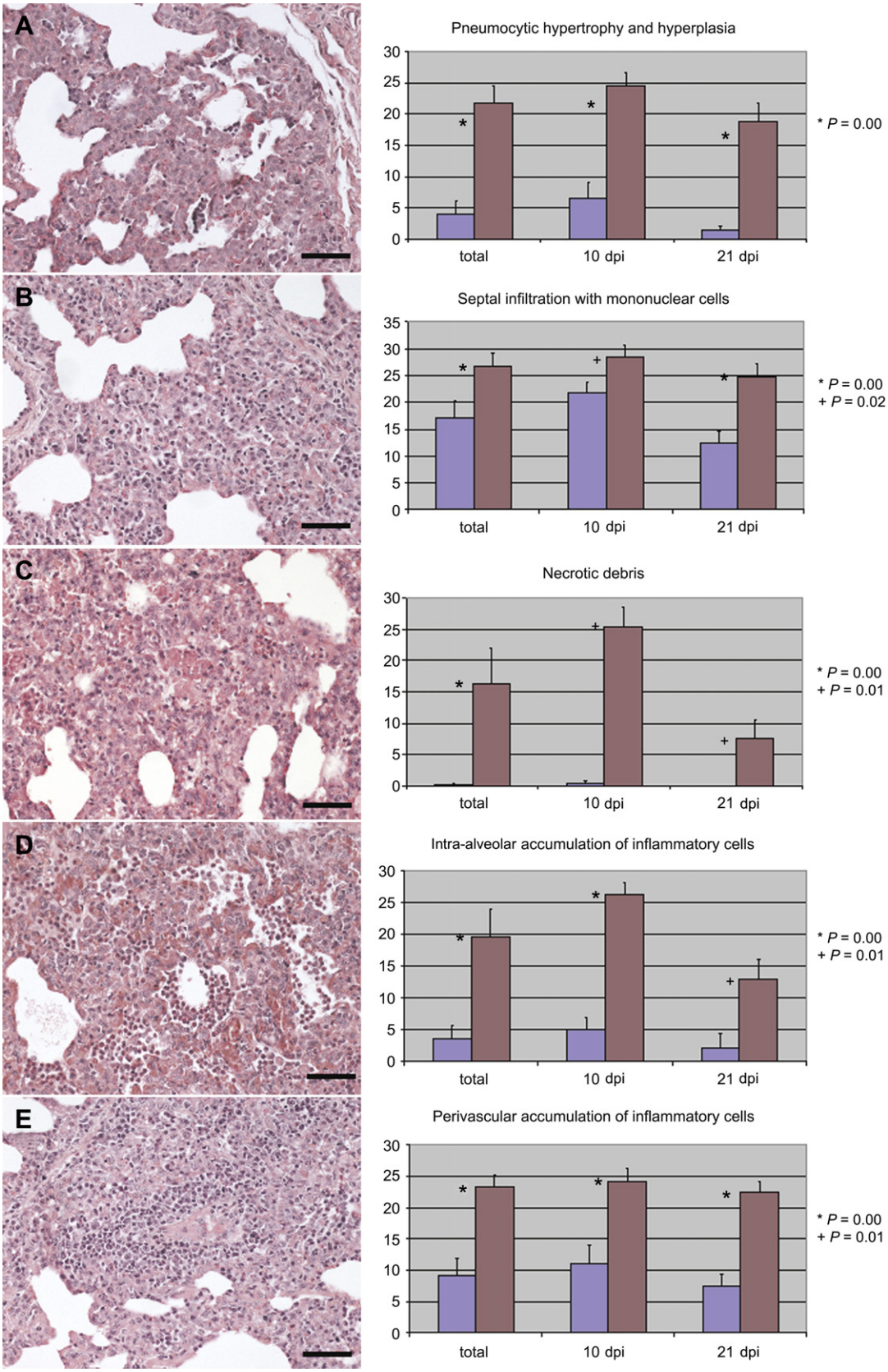

Fig. 1. The five parameters that were scored on HE-stained slides. (A) Pneumocyte hypertrophy and hyperplasia. (B) Septal mononuclear infiltration. (C) Intra-alveolar necrotic debris. (D) Intra-alveolar inflammatory cell accumulation. (E) Perivascular inflammatory cell accumulation. HE. Bars, 50 μm. Adjacent to each image, the diagrams show the scores at 10 and 21 dpi and the sum of the scores at the two time points. Blue bars represent the control animals and purple bars show the infected animals.

Please cite this article in press as: Balka G, et al., Immunohistochemical Characterization of Type II Pneumocyte Proliferation after Challenge with Type I Porcine Reproductive and..., Journal of Comparative Pathology (2013), http://dx.doi.org/10.1016/j.jcpa.2012.12.006

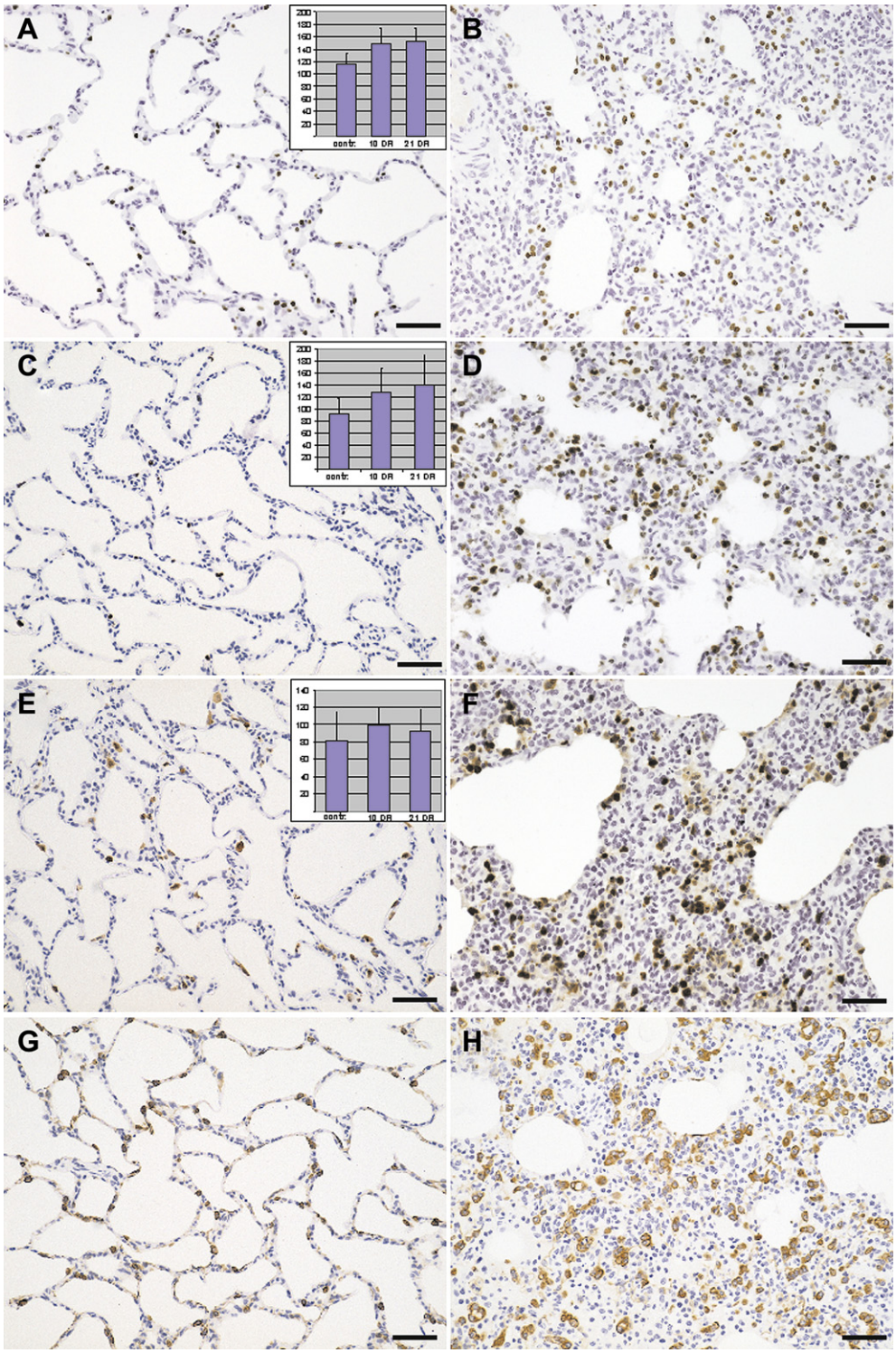

Fig. 2. Immunohistochemical labelling. (A) TTF-1 labelling of control lung. (B) TTF-1 labelling of infected lung. (C) Ki67 labelling of control lung. (D) Ki67 labelling of infected lung. (E) MAC387 labelling of control lung. (F) MAC387 labelling of infected lung. (G) Cytokeratin labelling of control lung. (H) Cytokeratin labelling of infected lung. Bars, 50 μm. The insets show the results (mean values and standard deviations) of the cell counts performed on the slides.

Please cite this article in press as: Balka G, et al., Immunohistochemical Characterization of Type II Pneumocyte Proliferation after Challenge with Type I Porcine Reproductive and..., Journal of Comparative Pathology (2013), http://dx.doi.org/10.1016/j.jcpa.2012.12.006

while extensive lung tissue damage is caused by the release of harmful substances from virus-infected macrophages (e.g. tumour necrosis factor [TNF]-α, other apoptogenic cytokines, reactive oxygen species and nitric oxide [NO]) (Choi *et al*., 2001; Choi and Chae, 2002; Kim *et al*., 2002; Labarque *et al*., 2003; Miller and Fox, 2004; Lee and Kleiboeker, 2007). After the initial, acute stage of the disease, and in the absence of secondary bacterial infection, the immune system and natural healing mechanisms remove the necrotic tissue, neutrophils disappear, alveoli are freed of content and damaged pneumocytes are replaced by proliferating type II pneumocytes.

In HE-stained tissue sections, type II pneumocytes are similar in appearance to activated macrophages; both have large, round or oval, euchromatic nuclei and abundant cytoplasm sometimes filled with numerous vesicles (surfactant material in the pneumocytes, phagosomes in the macrophages), and both may be present in abundant number in PRRS-affected lungs. The initial aim of the present study was to develop a means of identification of type II pneumocytes by testing the cross-reactivity of humanized anti-TTF-1 antibody.

TTF-1 is a nuclear homeodomain transcription factor that was originally described as a regulator of the thyroid-specific transcription of thyroglobulin, thyroperoxidase and thyrotropin receptor. In the lung, TTF-1 regulates developmental, cellular growth and differentiation processes and also surfactant gene and Clara cell secretory protein gene transcription (Bohinski *et al*., 1994; Ray *et al*., 1996; Zhou *et al*., 1996; Cai *et al*., 2001; Nakamura *et al*., 2002). Anti-TTF-1 antibody is widely used in human pathology for the identification and/or differentiation of primary or metastatic lung and thyroid carcinomas (Cai *et al*., 2001; Nakamura *et al*., 2002; Tan *et al*., 2003; Hirsch *et al*., 2004).

The TTF-1 antibody successfully identified type II pneumocytes with homogenous, intense, nuclear labelling. Labelled cells were located typically at the insertion of the alveolar spaces in the control lung samples. Bronchiolar epithelial cells were also labelled; however, non-ciliated Clara cells showed slightly stronger nuclear positivity. A similar distribution of TTF-1-positive bronchiolar cells is reported in human lung (Nakamura *et al*., 2002). As ciliated bronchiolar cells are related closely to non-ciliated Clara cells, the positive labelling of these cell types might suggest that TTF-1 has an effect on the function and/or development of both of these cells. In this context, as the authors suggest, TTF-1 might contribute to the maintenance of bronchiolar cell differentiation (Nakamura *et al*., 2002). Bronchiolar epithelial cells of similar TTF-1 labelling pattern and distribution have also been described in ovine lung (Beytut, 2010).

The number of type II pneumocytes was enumerated, but TTF-1-positive bronchiolar cells were not included in these calculations. Statistical analysis revealed that the number of positively labelled cells increased significantly in infected animals at 10 dpi compared with negative control animals and did not decrease by 21 dpi. The increase in these cells reflects extensive type I pneumocyte damage caused by direct and indirect ('bystander') effects of PRRSV replication. The study was terminated at 21 dpi and total histological healing was not observed, but the infected animals recovered from the clinical disease and the presence of type II pneumocytes in high number after inoculation in both early and late stages of the disease demonstrated their importance in lung healing. The most prominent feature of the resolution process in the lung was the almost total disappearance of the intra-alveolar necrotic debris and intra-alveolar inflammatory cell infiltration by 21 dpi. The presence of intra-alveolar necrotic debris and extensive type II pneumocyte proliferation is the main hallmark of a disease termed proliferative and necrotizing pneumonia (PNP), a frequent lung lesion in growing pigs that has been predominantly attributed to PRRSV, porcine circovirus (PCV)-2 and swine influenza virus (SIV) infections (Drolet *et al*., 2003; Grau-Roma and Segalés, 2007; Hansen *et al*., 2010; Morandi *et al*., 2010).

Ki67 labelling was used to assess mitosis, as Ki67 protein is present during all active phases of the cell cycle (G_1, S, G_2 and mitosis), but is absent from resting cells (G_0) (Scholzen and Gerdes, 2000). Up-regulation was readily observed, but was not statistically significant. MAC387-positive macrophages showed similar up-regulation without statistical significance. The relatively high variation in mean values between the individual PRRSV-infected animals indicates differences in response to infection, both in terms of macrophage infiltration and pneumocyte (and other cell) proliferation. The high standard deviation obtained for the individual parameters illustrates the variation in the number of labelled cells in different microscopical fields. This feature is in accord with routine histological findings, where different areas within the same slide also showed differences in the severity of lesions.

Cytokeratin labelling was performed to identify epithelial cells and to compare the shape and location of type I and II pneumocytes. The findings were in agreement with studies describing human alveolar epithelial cell structures (Fehrenbach, 2000). This labelling was not suitable for cell counting as there was

Please cite this article in press as: Balka G, et al., Immunohistochemical Characterization of Type II Pneumocyte Proliferation after Challenge with Type I Porcine Reproductive and..., Journal of Comparative Pathology (2013), http://dx.doi.org/10.1016/j.jcpa.2012.12.006

insufficient difference to allow differentiation between pneumocyte types.

There were few PRRSV antigen-positive cells at 10 dpi and none at 21 dpi. This finding agrees with the observations of Gómez-Laguna *et al.* (2010), who observed a peak in the presence of PRRSV antigen in the lung tissues at 7 dpi followed by a marked decrease by 10 dpi and almost total absence by 21 dpi.

A further aim of the present study was to determine whether there was correlation between the number of TTF-1-positive type II pneumocytes, Ki67-positive proliferating cells, MAC387-positive macrophages and the histological severity of the lung lesions. The goal of these investigations was to find an objective immunohistochemical method that could replace the subjective scoring system. In this context, the number of Ki67-labelled cells was correlated with overall severity of lung lesions ($P < 0.05$, $r = 0.503$). As the correspondence between the two values was not linear, despite the positive correlation, the values were not interchangeable.

The number of TTF-1-positive type II pneumocytes showed a significant ($P < 0.05$) increase at 10 dpi in infected pigs. Despite overall increases in the mean values for Ki67 and MAC387 labelling, relatively high standard deviations negated their statistical significance. When comparing cell counts after the different labelling methods, marked individual differences between the animals within the same groups may have contributed to the differences observed in clinical signs and pathological lesions.

Conventional animals were selected in order to imitate field infection more accurately. Despite this, the possibility remains that individual differences, high rates of standard deviation and non-linear correspondence between the correlating values (Ki67 and histological severity) can be attributed to the fact that conventional PRRSV-free pigs (rather than specific pathogen free animals) were used in the study.

Acknowledgments

This paper was supported by the János Bolyai Research Scholarship of the Hungarian Academy of Sciences, by the TÁMOP-4.2.2.B-10/1 and TÁMOP-4.2.1.B-11/2/KMR-2011-0003 grants. We would like to thank C. Duignan for his grammatical suggestions.

References

Beytut E (2010) Sheep pox virus induces proliferation of type II pneumocytes in the lungs. *Journal of Comparative Pathology*, **143**, 132–141.

Bohinski RJ, DiLauro R, Whitsett JA (1994) Lung-specific surfactant protein B gene promoter is a target for thyroid transcription factor 1 and hepatocyte nuclear factor 3 indicating common mechanisms for organ-specific gene expression along the foregut axis. *Molecular and Cellular Biology*, **14**, 5671–5681.

Cai YC, Banner B, Glickman J, Odze RD (2001) Cytokeratin 7 and 20 and thyroid transcription factor 1 can help distinguish pulmonary from gastrointestinal carcinoid and pancreatic endocrine tumors. *Human Pathology*, **32**, 1087–1093.

Caswell CL, Williams KJ (2007) Respiratory system. In: *Jubb, Kennedy, and Palmer's Pathology of Domestic Animals*, 5th Edit., MG Maxie, Ed., Saunders Elsevier, Philadelphia, pp. 523–653.

Choi C, Chae C (2002) Expression of tumour necrosis factor-alpha is associated with apoptosis in lungs of pigs experimentally infected with porcine reproductive and respiratory syndrome virus. *Research in Veterinary Science*, **72**, 45–49.

Choi C, Cho W-S, Kim B, Chae C (2001) Expression of interferon-gamma and tumour necrosis factor-alpha in pigs experimentally infected with porcine reproductive and respiratory syndrome virus (PRRSV). *Journal of Comparative Pathology*, **127**, 106–113.

Crapo JD, Barry BE, Gehr P, Bachofen M, Weibel ER (1982) Cell number and cell characteristics of the normal human lung. *American Review of Respiratory Disease*, **126**, 332–337.

Drolet R, Larochelle R, Morin M, Delisle B, Magar R (2003) Detection rates of porcine reproductive and respiratory syndrome virus, porcine circovirus type 2, and swine influenza virus in porcine proliferative and necrotizing pneumonia. *Veterinary Pathology*, **40**, 143–148.

Fehrenbach H (2000) Alveolar epithelial type II cell: defender of the alveolus revisited. *Respiratory Research*, **2**, 33–46.

Gómez-Laguna J, Salguero FJ, Barranco I, Pallarés FJ, Rodriguez-Gómez IM *et al.* (2010) Cytokine expression by macrophages in the lung of pigs infected with the porcine reproductive and respiratory syndrome virus. *Journal of Comparative Pathology*, **142**, 51–60.

Grau-Roma L, Segalés J (2007) Detection of porcine reproductive and respiratory syndrome virus, porcine circovirus type 2, swine influenza virus and Aujeszky's disease virus in cases of porcine proliferative and necrotizing pneumonia (PNP) in Spain. *Veterinary Microbiology*, **119**, 144–151.

Halbur PG, Paul PS, Meng XJ, Lum MA, Andrews JJ *et al.* (1996) Comparative pathogenicity of nine US porcine reproductive and respiratory syndrome virus (PRRSV) isolates in a five-week-old cesarean-derived, colostrum-deprived pig model. *Journal of Veterinary Diagnostic Investigation*, **8**, 11–20.

Halbur PG, Paul PS, Meng XJ, Lum MA, Eernisse K *et al.* (1995) Comparison of the pathogenicity of two US porcine reproductive and respiratory syndrome virus isolates with that of the Lelystad virus. *Veterinary Pathology*, **32**, 648–660.

Hansen MS, Pors SE, Jensen HE, Bile-Hansen V, Bisgaard M *et al*. (2010) An investigation of the pathology and pathogens associated with porcine respiratory disease complex in Denmark. *Journal of Comparative Pathology*, **143**, 120–131.

Hirsch MS, Faquin WC, Krane JF (2004) Thyroid transcription factor-1, but not p53, is helpful in distinguishing moderately differentiated neuroendocrine carcinoma of the larynx from medullary carcinoma of the thyroid. *Modern Pathology*, **17**, 631–636.

Karniychuk UU, Geldhof M, Vanhee M, Van Doorsselaere J, Saveleva TA *et al*. (2010) Pathogenesis and antigenic characterization of a new East European subtype 3 porcine reproductive and respiratory syndrome virus isolate. *BMC Veterinary Research*, **6**, 30.

Kim TS, Benfield DA, Rowland RR (2002) Porcine reproductive and respiratory syndrome virus-induced cell death exhibits features consistent with a non-typical form of apoptosis. *Virus Research*, **85**, 133–140.

Labarque G, Van Gucht S, Nauwynck H, Van Reeth K, Pensaert M (2003) Apoptosis in the lungs of pigs infected with porcine reproductive and respiratory syndrome virus and associations with the production of apoptogenic cytokines. *Veterinary Research*, **34**, 249–260.

Lee SM, Kleiboeker SB (2007) Porcine reproductive and respiratory syndrome virus induces apoptosis through a mitochondria-mediated pathway. *Virology*, **365**, 419–434.

Miller LC, Fox JM (2004) Apoptosis and porcine reproductive and respiratory syndrome virus. *Veterinary Immunology and Immunopathology*, **102**, 131–142.

Morandi F, Ostanello F, Fusaro L, Bacci B, Nigrelli A *et al*. (2010) Immunohistochemical detection of aetiological agents of proliferative and necrotizing pneumonia in Italian pigs. *Journal of Comparative Pathology*, **142**, 74–78.

Nakamura N, Miyagi E, Murata SI, Kawaoi A, Katoh R (2002) Expression of thyroid transcription factor-1 in normal and neoplastic lung tissues. *Modern Pathology*, **15**, 1058–1067.

Nelsen CJ, Murtaugh MP, Faaberg KS (1999) Porcine reproductive and respiratory syndrome virus comparison: divergent evolution on two continents. *Journal of Virology*, **73**, 271–280.

Ray MK, Chen CY, Schwarts RJ, DeMayo FJ (1996) Transcription regulation of a mouse Clara cell-specific protein (mCC10) gene by the Nkx transcription factor family members thyroid transcription factor 1 and cardiac muscle-specific homeobox protein (CSX). *Molecular and Cellular Biology*, **16**, 2056–2064.

Rossow KD (1998) Porcine reproductive and respiratory syndrome. *Veterinary Pathology*, **35**, 1–20.

Scholzen T, Gerdes J (2000) The Ki-67 protein: from the known and the unknown. *Journal of Cellular Physiology*, **182**, 311–322.

Stadejek T, Oleksiewicz MB, Scherbakov AV, Timina AM, Krabbe JS *et al*. (2008) Definition of subtypes in the European genotype of porcine reproductive and respiratory syndrome virus: nucleocapsid characteristics and geographical distribution in Europe. *Archives of Virology*, **153**, 1479–1488.

Tan D, Li Q, Deeb G, Ramnath N, Slocum HK *et al*. (2003) Thyroid transcription factor-1 expression prevalence and its clinical implications in non-small cell lung cancer: a high-throughput tissue microarray and immunohistochemistry study. *Human Pathology*, **34**, 597–604.

Zhou L, Lim L, Costa RH, Whitsett JA (1996) Thyroid transcription factor-1 hepatocyte nuclear factor-3beta, surfactant protein B, C, and Clara cell secretory protein in developing mouse lung. *Journal of Histochemistry and Cytochemistry*, **44**, 1183–1193.

Zimmerman JJ, Benfield DA, Dee SA, Murtaugh MP, Stadejek T *et al*. (2012) Porcine reproductive and respiratory syndrome virus (porcine arterivirus). In: *Diseases of Swine*, 10th Edit., JJ Zimmerman, LA Karriker, A Ramirez, KJ Schwartz, GW Stevenson, Eds., Wiley-Blackwell, Hoboken, pp. 461–486.

[*Received, September 15th, 2012*
Accepted, December 19th, 2012]